Electronic Supplementary Material (ESI) for Physical Chemistry Chemical Physics.
This journal is © the Owner Societies 2015

Self-assembled trityl radical capsules. Implications for Dynamic Nuclear Polarization

Ildefonso Marin-Montesinos, Juan Carlos Paniagua, Marta Vilaseca, Ainhoa Urtizberea, Fernando Luis, Miguel Feliz, Feng Lin, Sabine Van Doorslaer, Miquel Pons*

Supplementary information

Figure S1. UV-Vis spectra of OX63 at 5 μM, 500 μM and 5 mM.

Figure S2. TMA binding to 10 μM OX63 (monomeric) followed by a decrease in the apparent molar absorption coefficient.

Figure S3. Concentration dependency of ESI-MS of OX63 in water.

Figure S4. Comparison of X-band CW spectra of 1.5 mM and 15 mM OX63 solutions measured at 40K to minimize saturation in 1:1 glycerol:D_2O and 1 M TMA.

Figure S5. Comparison of X-band CW-EPR spectra of a 1:1 glycerol:D_2O solution of 15 mM OX63 with and without 1M TMA.

Figure S6. Simulated contribution of S=1 system and comparison with experimental X-band CW-EPR spectra

Figure S7. Iso-spin-density surface of the dome conformation of OX63 monomer.

Figure S8. Effect of annealing on the EPR saturation behavior of 15 mM OX63 with and without TMA.

Figure S9. Temperature stability controls for SQUID magnetization experiments

Figure S10. Polarization buildup of 1M ^{13}C-TMA in presence of 30 mM OX63 in glycerol-water (1:1) at 1.4K.

Figure S11. Schematic representation of the DNP annealing experiment.

Figure S12. X-band CW-EPR spectra of a 1:1 glycerol:D_2O solution of 1M choline and 15 mM OX63 measured at 2.8 K.

Figure S13. X-band CW-EPR spectra (half-field signal) of a 1:1 glycerol:D_2O solution of 1M choline and 15 mM OX63 measured at 2.8 K.

Figure S14. Effect of annealing on the EPR saturation behavior of 15 mM OX63 with 1M choline.

Table S1. Calculated isotropic hyperfine couplings in OX63 monomer and dimer.

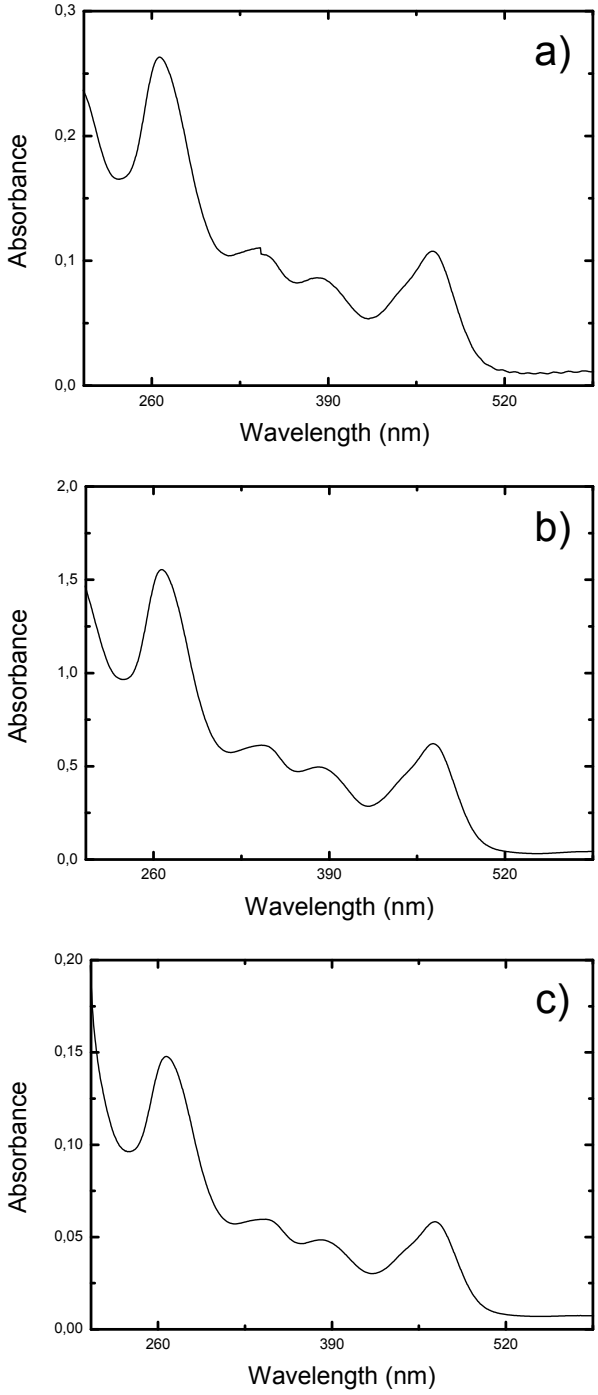

Figure S1. UV-Vis spectra of OX63 measured at 298K in degassed 10 mM phosphate buffer, pH 7 at OX63 concentrations and cuvette path lengths of a) 5 mM (l=0,001 cm), b) 500 μM (l=0,1 cm), and c) 5 μM (l= 1 cm).

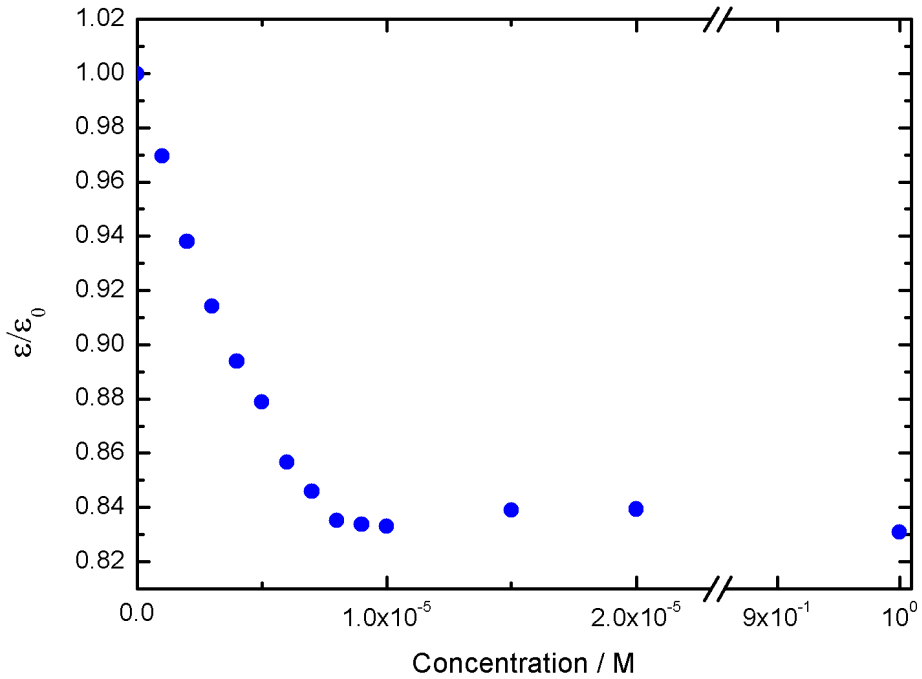

Figure S2. Titration of a 10 μM sample of OX63 with TMA followed by the relative change in the apparent molar absorption coefficient.

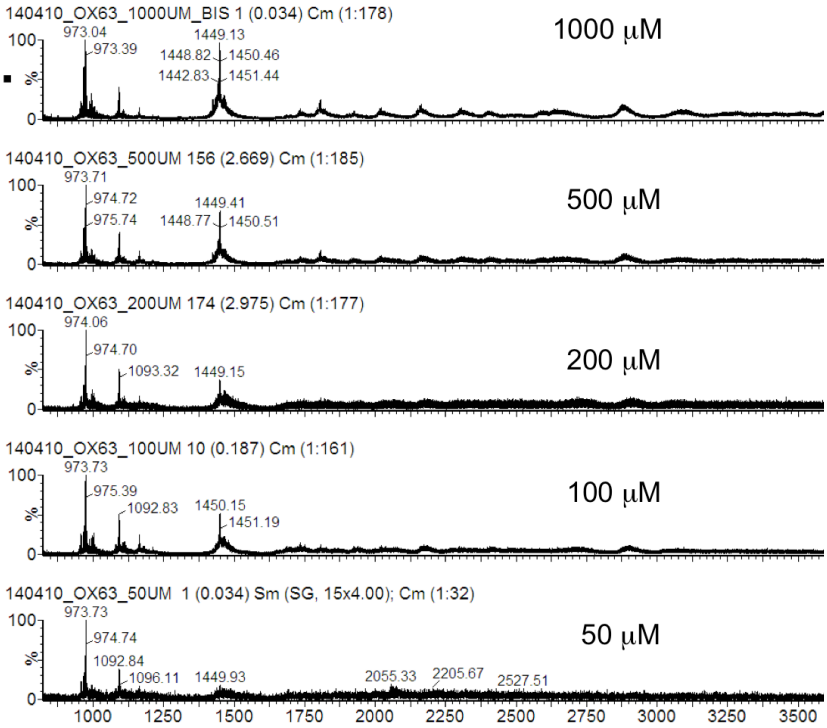

Figure S3. ESI-MS spectra of OX63 injected at the indicated concentrations in water.

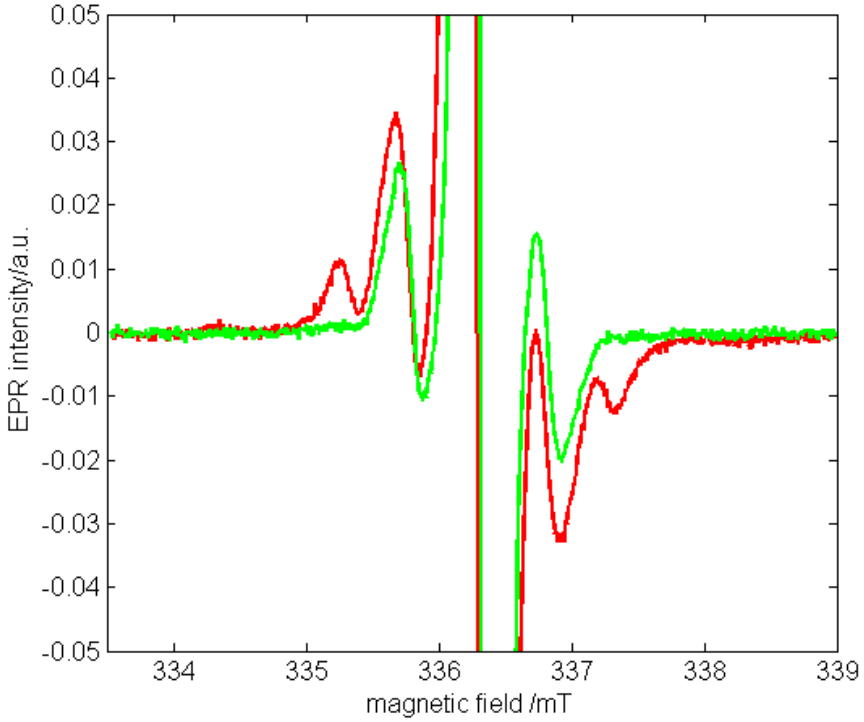

Figure S4. X-band CW-EPR spectra of 1:1 glycerol:D_2O solutions of 1M TMA and 15 mM OX63 (red) or 1.5 mM OX63 (green) recorded at 40K to minimize signal saturation effects.

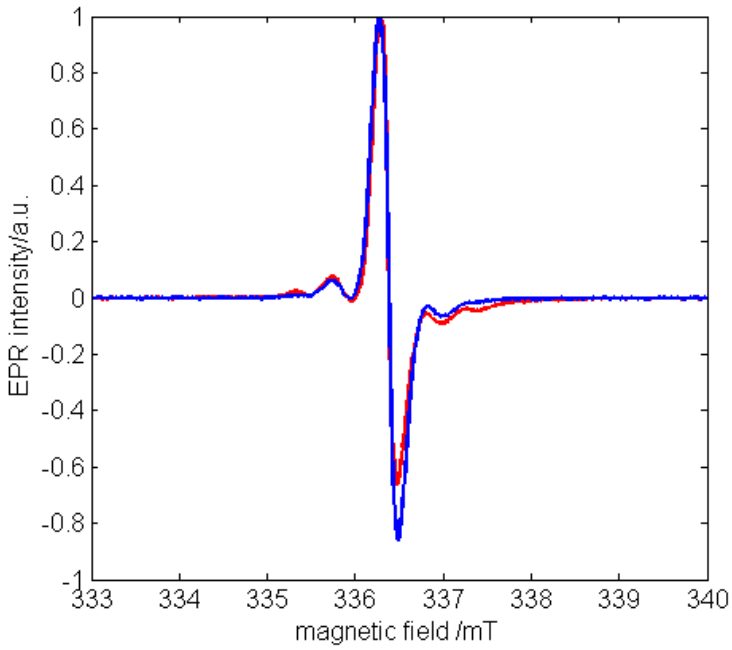

Figure S5. Comparison of X-band CW-EPR spectra of a 1:1 glycerol:D_2O solutions of 15 mM OX63 with (red) and without (blue) 1M TMA. The spectra were recorded with a microwave power of 250 nW at 2.8 and 2.5 K, respectively.

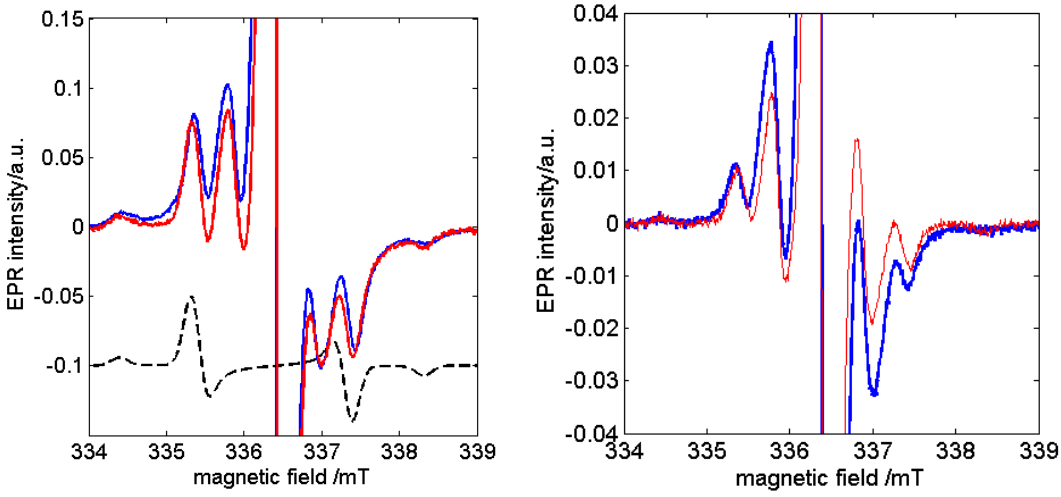

Figure S6. Comparison of simulated and experimental X-band CW-EPR spectra. The black dotted line is the simulation of a S=1 system with *D*=55 MHz and g=2.003 done with the EasySpin program [S. Stoll, A. Schweiger, J. Magn. Reson., 178, 42-55 (2006)]. Left panel. Comparison of experimental spectra of 30 mM OX63 (blue) and simulated spectra (red) obtained by adding the contribution from the S=1 system to the experimental spectra of 15 mM OX63. Right panel. Comparison of experimental spectra of 15 mM OX63 (blue) and simulated spectra (red) obtained by adding the contribution from the S=1 system to the experimental spectra of 1.5 mM OX63.

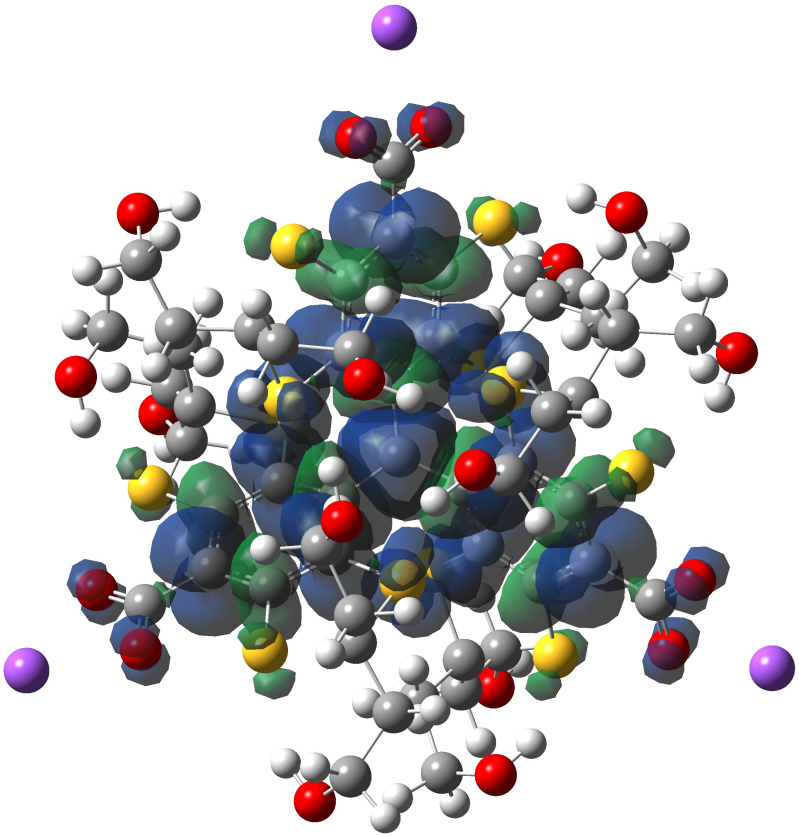

Figure S7: Iso-spin-density surface of the dome-shape conformation of the OX63 monomer corresponding to ±0.0004 au. The spin-density map was represented with Gauss View IM version 5.0.9 [R. Dennington, T. Keith and J. Millam, Semichem Inc., Shawnee Mission KS, 2009].

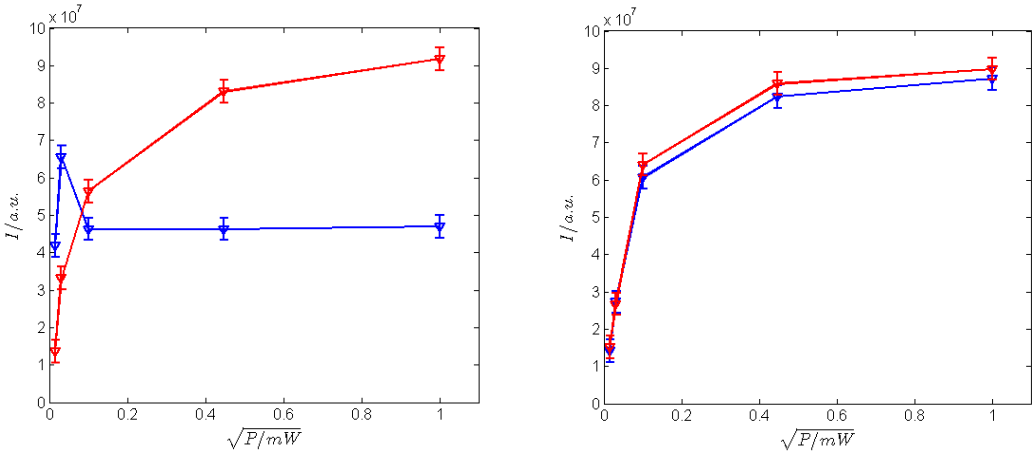

Figure S8. Plots of double integral of CW-EPR spectra versus the square root of the microwave power for 1:1 glycerol:D_2O solutions of 15mM OX63 with 1 M of TMA (left, T=2.6K) and without TMA (right, T=2.5K). The samples were evacuated to 1 mbar to remove excess O_2. The blue curves show the saturation observed immediately after cooling from room temperature. The red curves show the intensity behavior after cooling, 30' annealing at 5 K and re-cooling to the set temperature. The saturation behavior clearly is affected by annealing in the presence of TMA but not in pure OX63.

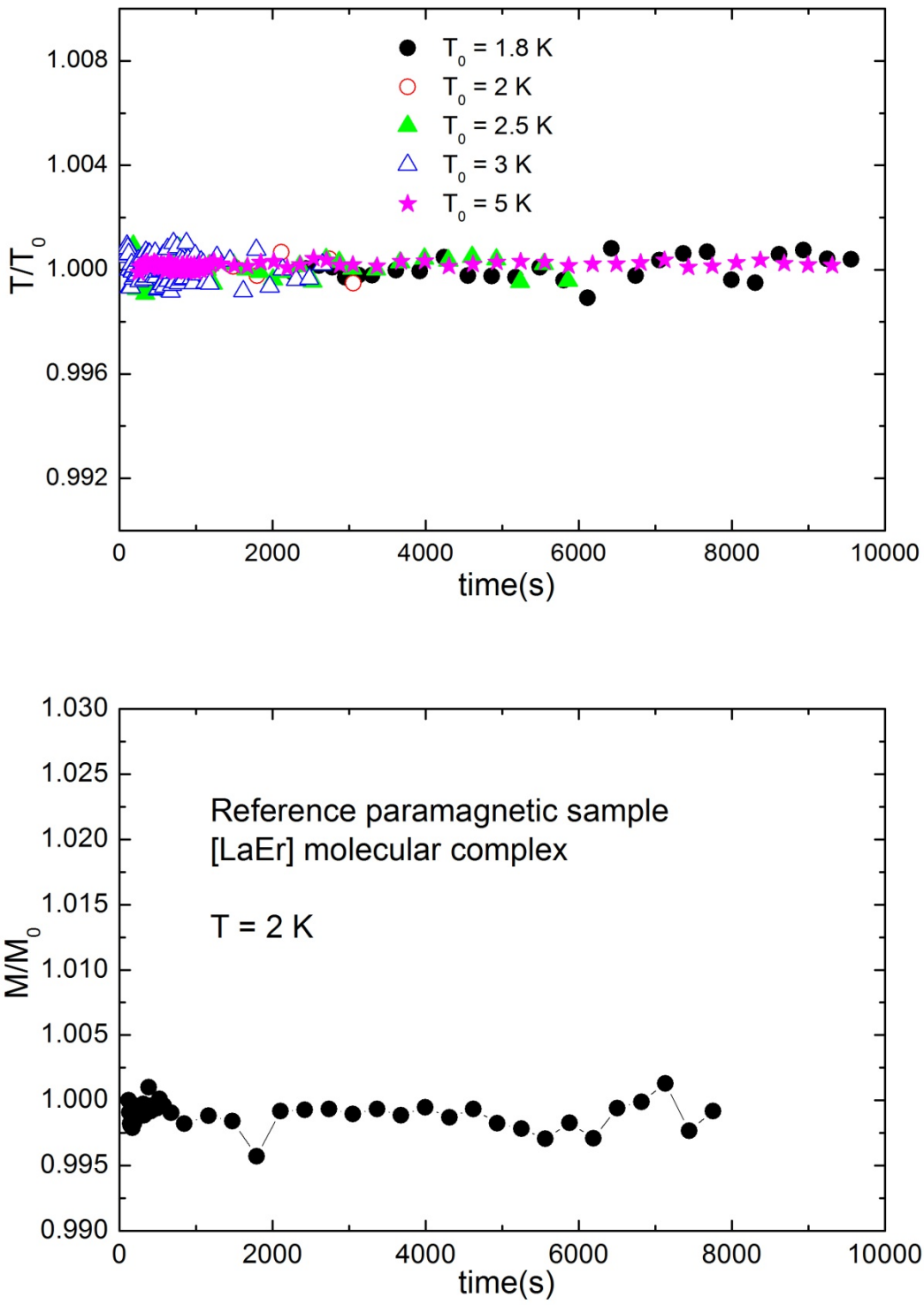

Figure S9. (top) Thermal stability of magnetic relaxation experiments performed at several average temperatures T_0. (bottom) Relaxation of the magnetization of a standard paramagnetic sample measured at 2 K using the same experimental protocol followed in the case of OX63 samples (Fig. 6).

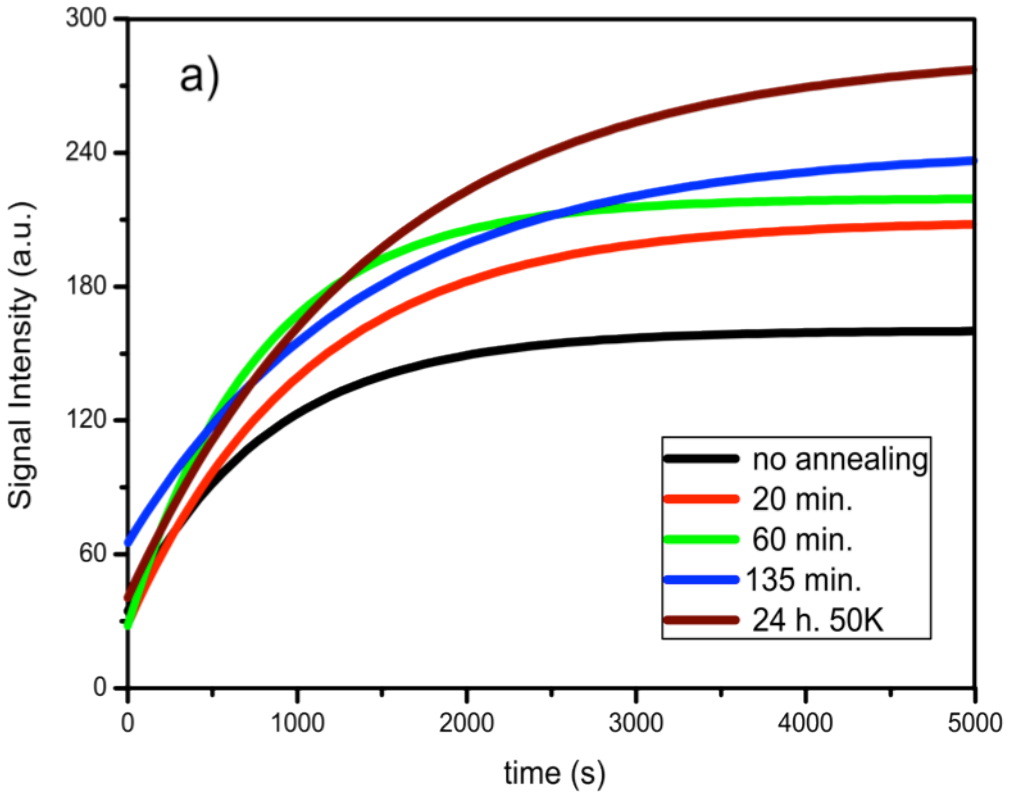

Figure S10. Polarization buildup of 1M ^{13}C-TMA in presence of 30 mM OX63 in glycerol-water (1:1) at 1.4K. The samples were first cooled to 1.4K, warmed to 2K and maintained at this temperature for the indicated times. Finally they were cooled down again to 1.4 K before polarization was started. The protocol is shown schematically in Figure S7. As a reference the polarization buildup under the same conditions of samples directly cooled to 1.4 K (no annealing) or annealed at 50K for 24h are shown.

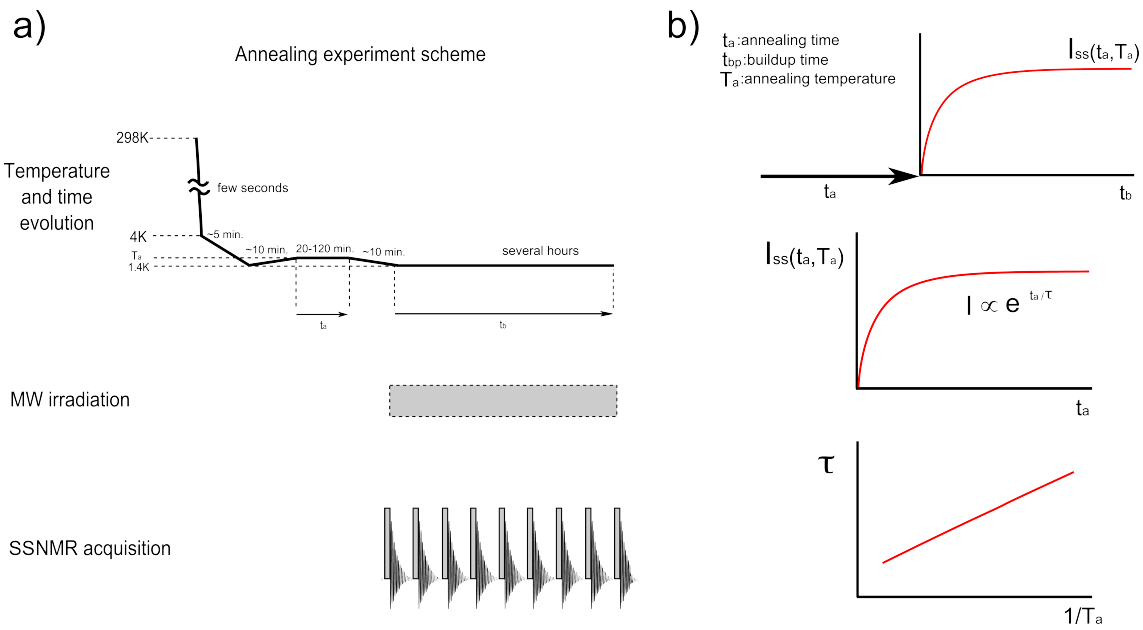

Figure S11. Schematic representation of the DNP annealing experiment. a) Time course of the experiment and definition of the various times (t) and temperatures (T). b) Schematic representation of the exponential processes observed. Typical polarization buildup curves are shown in Figure S8. The steady state polarization increases exponentially as a function of the annealing time (t_a) as shown in Figure 7 of the main text. For each annealing temperature (T_a) the time constant of the annealing process (τ) was determined by least-square fitting of the exponential. The Arrhenius plot shown schematically in the bottom graph is shown in Figure 6c.

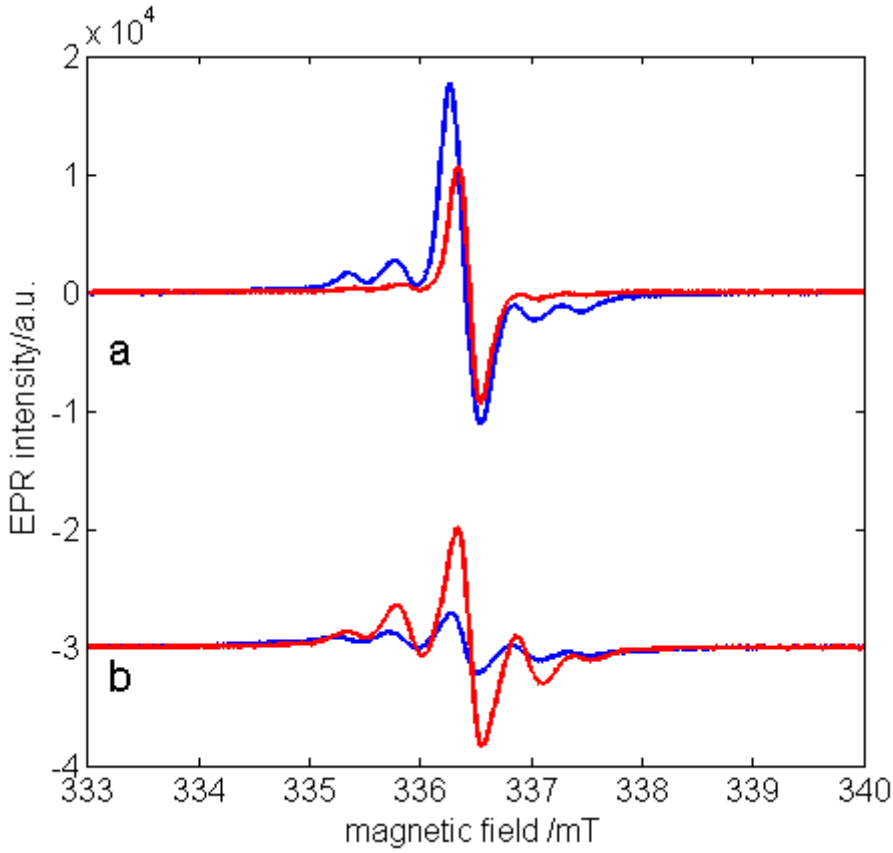

Figure S12. X-band CW-EPR spectra of a 1:1 glycerol:D_2O solution of 1M choline and 15 mM OX63 measured at 2.8 K using a microwave power of (a) 1μW and (b) 1mW. The EPR signals are taken directly after cooling to 2.8 K (blue), and after a 30 minutes annealing at 5 K (red).

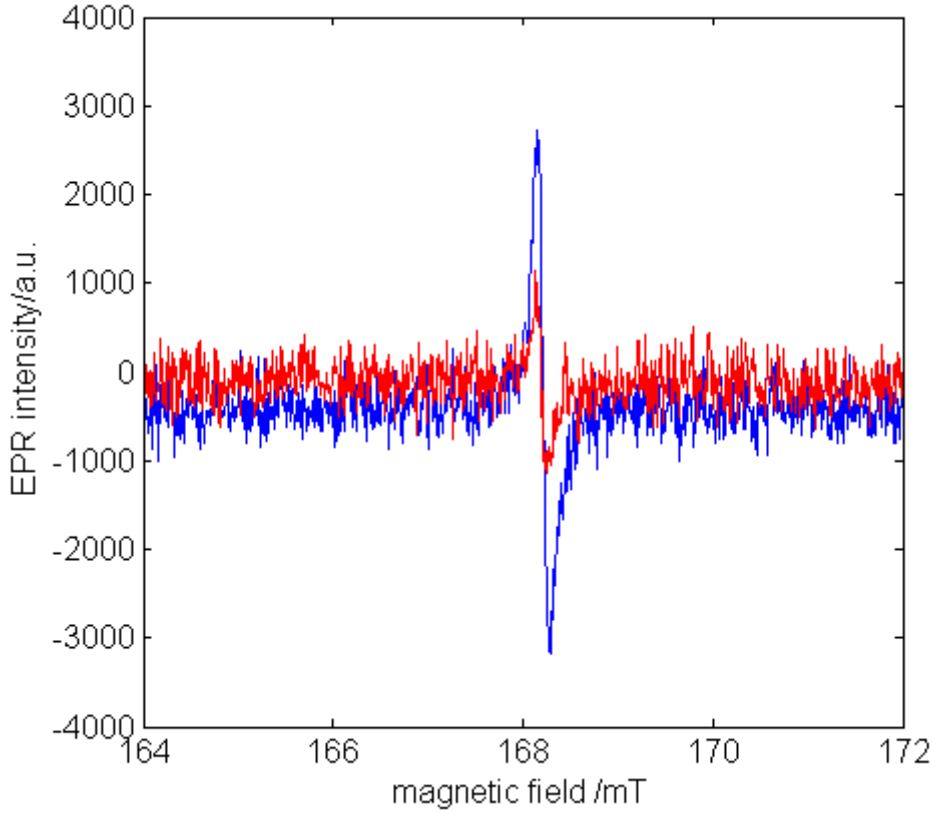

Figure S13. X-band CW-EPR spectra (half-field signal) of a 1:1 glycerol:D_2O solution of 1M choline and 15 mM OX63 measured at 2.8 K with a microwave power of 200 μW. The EPR signals are taken directly after cooling to 2.8 K (blue), and after a 30 minutes annealing at 5 K (red).

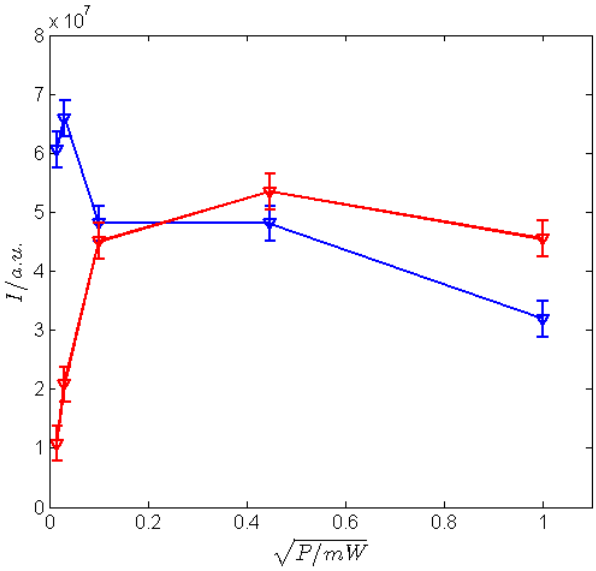

Figure S14. Plot of double integral of CW-EPR spectra versus the square root of the microwave power for a 1:1 glycerol:D_2O solution of 15mM OX63 with choline. The spectra are recorded at 2.5 K and the sample tube was evacuated to 1mbar to remove excess O_2. The blue curve shows the saturation after immediate cooling from room temperature to 2.5K, the red curve shows the intensity behavior after a subsequent annealing of 30' at 5 K and re-cooling to 2.5 K. The saturation behavior has clearly changed.

Table S1. in MHz for the carbon atoms of OX63 monomer and dimer (see the experimental section for computational details).

Atom	Monomer	Dimer	Dimer with TMA
Central	58.9	29.8	29.4
Ipso	−31.8	−15.9	−15.8
Ortho	21.9, 29.2	10.8, 14.5	10.8, 14.8
Meta	−6.6, −9.1	−3.2, −4.5	−3.3, −4.5
Para	9.3	4.6	4.6
Carboxyl	−3.8	−1.9	−1.9